Запропоновано методику аналізу довговічності несучих валів ексцентрикових механізмів на основі скінченно-елементного моделювання. При проведенні аналізу досліджується усталений рух механізму. Аналіз довговічності базується на моделі адитивного накопичення пошкоджень. Оцінка напружень у валу проводиться на базі скінченно-елементного моделювання функціонування механізму в усталеному режимі на робочих частотах, які є найближчими до критичних. Після виявлення концентраторів напружень та найнапруженіших ділянок валу проводиться аналіз характерного циклу навантаження. Після зведення циклу навантаження до низки симетричних циклів проводиться оцінка пошкодження валу на кожному циклі та його ресурсу.

На базі запропонованого методу проведено аналіз довговічності несучого валу центробіжно-гіраційного рудного млину кулісного типу. На базі механічної моделі з метою підвищення ефективності та швидкодії скінченно-елементного розрахунку побудовано спрощену розрахункову модель. Запропоновано модель руху руди в помольних камерах при усталеному режимі руху. Побудовано діаграми Кемпбела коливань системи та виявлено, що механізм млину не входить до резонансу з робочою частотою збудження. Виявлено ділянку концентрації механічних напружень та ділянку максимальних механічних напружень у валу млину. Проведено аналіз умов функціонування валу та обчислено значення межі витривалості матеріалу валу в зоні найбільших напружень. Побудовано характерний цикл навантаження валу млина при усталеному режимі роботи, який складається з 16 ділянок. Кожну ділянку зведено до симетричного циклу, що дозволило обчислити пошкодження валу на кожній ділянці циклу та на всьому циклі навантаження в цілому. Застосування методики адитивного накопичення пошкоджень дозволило оцінити ресурс валу млина. Запропоновану методику оцінки довговічності несучого валу може бути використано для аналізу ресурсу різноманітних гірничопереробних механізмів, обладнання легкої промисловості та віброгенераторів

Ключові слова: ексцентриковий механізм, багатоциклова втома, скінченно-елементний аналіз, динамічні навантаження, діаграма Кемпбела

UDC 62-251
DOI: 10.15587/1729-4061.2019.174030

ESTIMATION OF DURABILITY OF CARRIER SHAFTS IN ECCENTRIC MECHANISMS

D. Arinova
Doctoral Student*
E-mail: d_arinova@mail.ru
B. Uspensky
PhD**
E-mail: Uspensky.kubes@gmail.com
K. Avramov
Doctor of Technical Sciences, Professor**
E-mail: kvavramov@gmail.com
V. Povetkin
Doctor of Technical Sciences, Professor*
E-mail: vv1940_povetkin@mail.ru
*Department of Industrial Engineering
Satbayev University
Satpaev str., 22a, Almaty,
Republic of Kazakhstan, 050013
**Department of Reliability
and Dynamic Strength
A. Pidgorny Institute of Mechanical
Engineering Problems of the National
Academy of Sciences of Ukraine
Pozharskoho str., 2/10, Kharkiv,
Ukraine, 61046

Received date 24.07.2019
Accepted date 07.10.2019
Published date 23.10.2019

1. Introduction

One of the main causes of failures of rotary mechanisms is the fatigue stresses of the carrying shaft. Analyzing such stresses, taking into consideration all the different loading features that arise from the operation of a machine, is a complex task that can rarely be solved by classical analytical or semi-analytical methods. Solving such a task at the design phase would increase the service life of a mechanism, thereby improving its durability and reliability. Therefore, it is a relevant task to devise a procedure for analyzing the multicycle fatigue of the shaft. The most conventional methodology for analyzing the dynamic stressed-deformable state of complex structures is the method of finite elements, which allows the detailed consideration of features of their geometry.

Many engineering offices involved in the design of machine-building structures try to replace experimental resource studies with numerical modeling. First, experimental research is extremely expensive. Second, modern finite-element software packages make it possible to carry out numerical simulation of extremely complicated engineering structures, which produces sufficiently reliable resource calculations.

A Weller fatigue curve is used for conducting resource calculations; it is obtained experimentally. Many factors, such as a material's properties, geometric heterogeneities, loading conditions, environmental conditions, influence the parameters of the Weller curve and, therefore, the fatigue durability of rotating shafts. Local points of stress concentrations are typically a source of fatigue breakdowns.

2. Literature review and problem statement

Paper [1] gives the experimentally-derived Weller curves for samples with circumference incisions at different coefficients for stress concentrations. Works [1–3] report studies into the effect of incisions and scratches on the fatigue destruction of samples under the influence of monoharmonic periodic load. Paper [4] experimentally shows that the main cause of fatigue breakdowns of a car carrier shaft are significant fluctuations in stresses in the regions of their concentration, which leads to the emergence and development of fatigue cracks.

During service time, rotating parts of machines are exposed to irregular cyclical loads. For this type of rotating machine parts, their durability can be assessed using two main approaches. Conventional fatigue analysis is performed in a temporal domain; this employs a cycle counting technique called the rain flow method [5]. Spectral fatigue analysis implies the construction of a density function of the probability of stress range [6]. When using a conventional approach, the complex history of loading a part is reduced to a series of damaging cycles [7], which could then be applied to calculate their cumulative damaging effect [8]. A brief overview of fatigue analysis methods is given in paper [9]. The prediction of durability of a rigidly fixed beam under the influence of single-axle and multiaxial loading using the rain flow method and a Dirlik formula is reported in studies [10, 11]. The applicability of approaches in the time and frequency domains for different mechanical components, as well as their relative advantages and disadvantages, are considered in work [12]. Paper [13] examines the durability of a wind turbine, which is assessed using the rain flow method and a Dirlik approach. In studies [7–13], fatigue durability is calculated using different spectral methods for numerically simulated or real vibrations of a part or a machine and is compared to durability calculated by conventional methods. However, the accuracy of methods formulated in both time and frequency domains can only be reliably confirmed by comparing the estimated service life with the service life obtained from experiments. Currently, industries use computer analysis to systematically design reliable structures [14].

The task of static analysis of a crank shaft was solved in paper [15] using a finite element approach with the most loaded regions of the shaft identified. Work [16] analyzed the fatigue of a crank shaft in the diesel engine operating at the rated frequency of 1,500 rpm. Study [17] experimentally shows that a rotor breaks most often when it is constantly rotated. A procedure for assessing the limit of the multicycle curved fatigue of a crank shaft is described in [18].

A significant drawback of studies reported in [14–18] is that the stressed-deformed state of a crank shaft is considered without taking into consideration the influence exerted by other rotating parts. Work [19] experimentally shows that the resource of a locomotive carrier shaft is significantly influenced by the attachments of wheelset pairs, bearings, and brakes. Fatigue cracks were observed in the places where the shaft was connected to these elements in the absence of noticeable defects of the material. The scientific literature pays little attention to computer analysis of shafts of eccentric mechanisms. The predominant method for studying the fatigue of eccentric mechanisms is a field experiment [4, 18, 19, 20–22]. Such studies can increase the cost of a structure, reducing its competitiveness. Therefore, it is expedient to undertake a research aimed at analyzing the durability and resource of the carrier shaft of eccentric mechanisms using computer simulation.

3. The aim and objectives of the study

The aim of this study is to devise a procedure for assessing the durability of the carrier shaft of an eccentric mechanism, which would make it possible to calculate the resource of such structures and to develop recommendations to prolong it.

To accomplish the aim, the following tasks have been set:

– to devise an approach to calculating the resource of carrier shafts of eccentric mechanisms;

– to apply this approach to studying the resource and the stressed-deformed state of a mill shaft.

4. Approach to calculating the resource of carrier shafts

We propose an approach to the numerical assessment of the resource of force transmissions in mechanisms and machines, which is based on a joint analysis of the dynamic stressed-deformable state of a structure and its resource. The durability of a carrier shaft in the centrifugal-gyration rocker mill, the type of CGM 140/320, is considered as an example.

To calculate the resource of carrier rotating shafts, the fields of dynamic equivalent stresses over its single rotation were determined. We have considered the case of shaft rotation at constant angular speed. The most loaded operation mode of a structure was analyzed. In this case, it was assumed that grinding chambers are fully loaded with ore. Thus, the stressed-deformable state for the most loaded case was investigated. Then there is a major assessment of the structure resource.

When calculating SDS, it was assumed that the material of a shaft is isotropic, without cracks and defects. The connection between stresses and deformations is described by the Hook law. Deformations and displacements are related via Cauchy linear formals. The stressed state of the structure was assessed by finite-element modeling. Particular attention in calculations was paid to regions with stress concentrators that occur in places where the geometry of the shaft changes.

To assess the durability of a shaft, the dynamic SDS is calculated and the resource is evaluated, which is expressed in the form of the following algorithm:

1. The finite-element dynamic SDS of the structure.

2. Analysis of linear resonance properties of the structure using the Campbell diagrams. Calculation of the shaft resource should be carried out at modes closest to resonant ones.

3. Identify the most characteristic cyclically changing SDS of the structure under the most loaded mode.

4. Analyze fatigue of the shaft based on the following algorithm:

4. 1. Split a cycle into sections of a simple shape.

4. 2. Reduce each section to an equivalent symmetrical cycle.

4. 3. Assess shaft damage at each section.

4. 4. Assess shaft fatigue over a single loading cycle.

4. 5. Evaluate shaft resource.

5. The resource and stressed-deformed state of the shaft of the mill CGM 140/320

We shall examine the stressed-deformable state and resource of the ore mill CGM 140/320 [23]. The mill's complete geometric model includes both moving parts and elements that attach it to a fixed base. The main fixed parts of the mill are the frame and the case with a rack. Moving parts

include a shaft with a counterweight, a link, and a carrier with grinding chambers (Fig. 1). This design enables complex flat motion of grinding chambers.

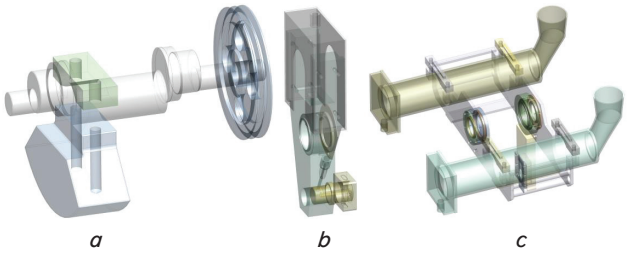

Fig. 1. Moving parts of the structure: *a* — shaft with a counterweight; *b* — link with a carrier pin and a block; *c* — carrier with grinding chambers

In the course of finite-element modeling of the mill movement, special attention is paid to the interaction between moving parts shown in Fig. 1.

5. 1. Model of the structure

The following assumptions were made when modeling the structure's dynamic SDS.

1. The dynamics of the mill's rotor are weakly influenced by its stationary parts, so the frame and body were not included in the finite-element analysis, except for the body bushings in which the rotor is installed.

2. Friction between parts of the machine was not taken into consideration.

3. Fixing the shaft in the bushings was considered absolutely rigid. Such an assumption increases the shaft stresses.

4. The contents of grinding chambers were considered a solid body.

The geometric model of the mill, taking into consideration the described assumptions, is shown in Fig. 2.

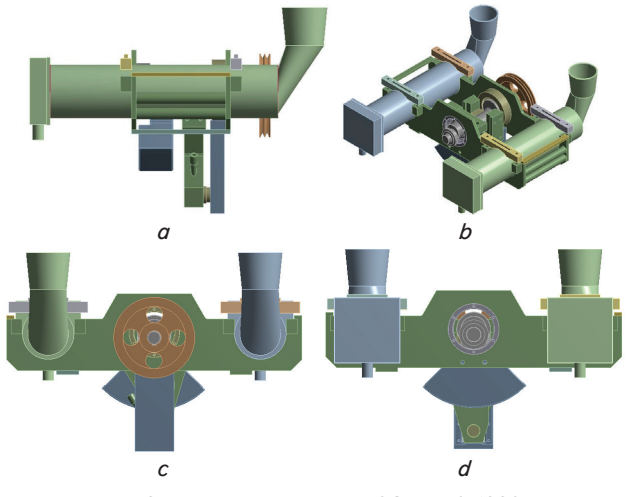

Fig. 2. Estimated model of CGM 140/320: *a* — side view; *b* — isometric projection; *c* — rear view; *d* — front view

The following materials that make up the main elements of the mill CGM 140/320 were accepted: shaft, carrier pin – steel 45; counterweight – steel 3; link – steel 20; grinding bodies and grinding chambers – steel 65G; block – bronze BROF 10-1-OST1-90054.

We examined effect of the load in the form of ore in grinding chambers on strength of the carrier shaft. Ore in grinding chambers was considered to be a solid body.

When modeling ore, we employed data on the bulk weight of barite ore with a grain size of 10 mm (1.42 kg/dm^3). Taking into consideration that the permissible load on grinding chambers is 30–40 %, we used a material that models ore, with a density of 0.568 kg/dm^3, which corresponds to the grinding chamber loading by 40 %.

To properly build a finite-element model of the mill and analyze the strength of its shaft, it is necessary to correctly assign connections and loads applied to the elements of the machine. The bushings that host the shaft are stationary and are rigidly attached to the body. Our calculations take into consideration the gravity force acting on bodies. The pulley's angular speed ω changes over time *t* in the following manner [24]:

$$\omega(t)=52\left(1-e^{-15t}\right)+780e^{-15t}\cdot t,\ \text{rad/s}, \quad (1)$$

where ω is the angular speed of the pulley; *t* is time.

The character of the shaft angular velocity over time is shown in Fig. 3.

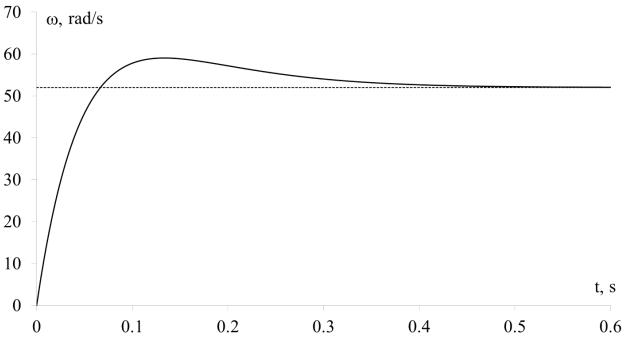

Fig. 3. Dependence graph of the shaft angular speed on time: ω — shaft angular speed, *t* — time

5. 2. Numerical simulation of resonance behavior

The finite-element modeling was employed to investigate the system's natural frequencies and oscillation forms at different values of angular speed of carrier shaft rotation. According to the results from modeling, a rapid enough convergence of results is achieved when using tetrahedral 3D finite elements. Moreover, these finite elements are good at approximating a region of the structure.

The shaft's oscillation calculations were carried out at a rated angular speed of its rotation, which corresponds to 30 rpm. According to the results from calculations, the torsional oscillations of the shaft occur in line with the first form (Fig. 4).

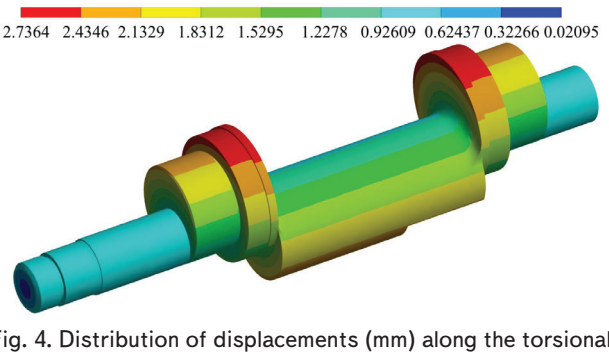

Fig. 4. Distribution of displacements (mm) along the torsional shape of shaft oscillations

Dependences of frequency of the system's natural oscillations on the angular speed of shaft rotation are shown in Fig. 5. Such dependences are termed the Campbell diagrams. Their analysis reveals that the system's natural oscillation frequencies are weakly dependent on the angular speed of shaft rotation in the range of $\omega \in [200; 800]$ rpm. There are no critical shaft frequencies over this range.

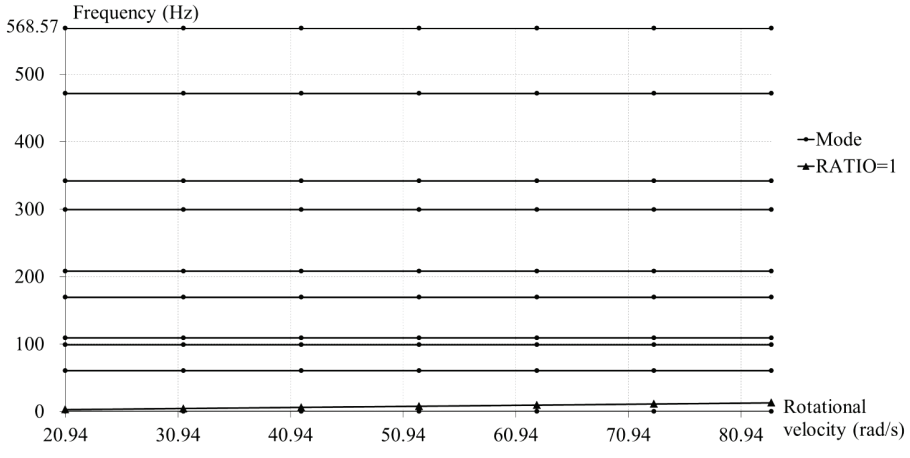

Fig. 5. Campbell diagram of the carrier shaft in the range of shaft angular velocities $\omega \in$ [200; 800] rpm

Thus, under conditions of regular operation of the mill there are no resonance phenomena.

5. 3. Dynamic SDS of the shaft

The dynamic SDS of the shaft was calculated over its five rotations at a constant angular speed of 500 rpm. The minimum and maximum distribution of dynamic equivalent shaft stresses are shown in Fig. 6, 7, respectively.

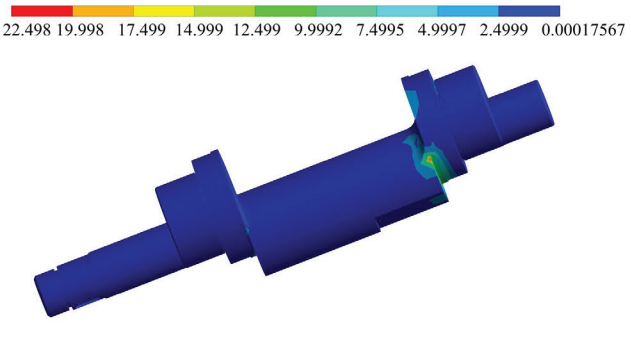

Fig. 6. Distribution of dynamic equivalent stresses (MPa) at a minimum magnitude of their values

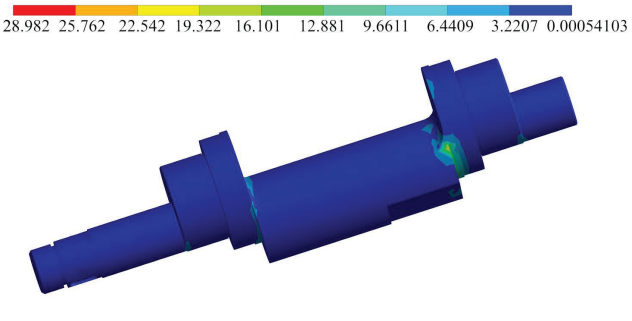

Fig. 7. Distribution of maximum equivalent dynamic stresses

Thus, the region on the cheek of the shaft near the crank is the most loaded. Therefore, analysis of the dynamic strength of the rotor comes down to analyzing the dynamic SDS in this loaded place.

It should be noted that at the beginning of motion, the system undergoes a short transition process. Studying the steady motion mode of the mill is carried out using simulation data that are at a distance of 3 from the onset of motion.

The yield limit of the shaft's material (steel 45) is 323 MPa; the strength limit is 540 MPa. Thus, the maximum stresses on the shaft under the steady motion mode of the mill at any kind of loading do not exceed 10 % of yield limit of the shaft's material. Results from calculating the dynamic SDS of the entire shaft are used to study its multi-cycle fatigue.

5. 4. Analysis of multi-cycle shaft fatigue

The character of dynamic equivalent stresses over time in the most loaded region of the shaft is shown in Fig. 8.

Thus, the cycle of equivalent stresses (Fig. 8) is asymmetrical and polyharmonic. Let us analyze fatigue of the shaft under such a load cycle according to the algorithm described above.

The dynamic process (Fig. 8) shall be divided into 16 asymmetrical cycles. As an example, a single cycle of equivalent stresses is shown in Fig. 9. Data on 16 asymmetric cycles are given in Table 1. It shows the maximum and minimum equivalent stresses in cycles in MPa.

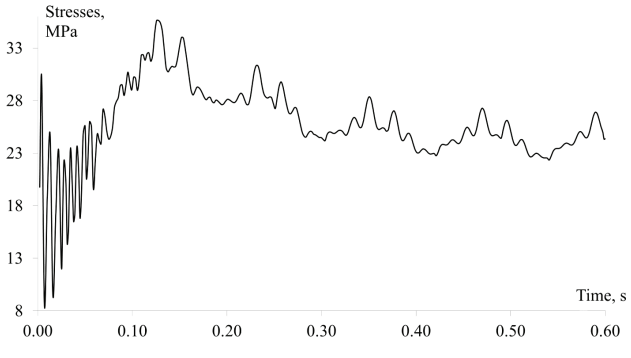

Fig. 8. Change in stress over time in the most loaded region

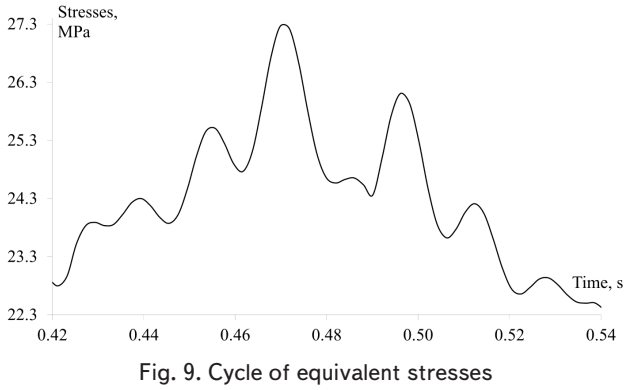

Fig. 9. Cycle of equivalent stresses

Table 1

Cycles of equivalent stresses

Section number	σ_{max}, MPa	σ_{min}, MPa
1	23.888	22.796
2	23.888	23.833
3	24.298	23.833
4	24.298	23.871
5	25.457	23.871
6	25.457	24.766
7	27.258	24.766
8	27.258	24.565
9	24.626	24.652
10	24.652	24.355
11	26.105	24.355
12	26.105	23.621
13	24.209	23.621
14	24.209	22.656
15	22.932	22.656
16	22.932	22.498

Damage to the shaft due to its loading at each section is calculated according to the damage summation rule [25]:

$$D=\sum_{i=1}^{16}\frac{1}{N_i}, \tag{2}$$

where N_i is the number of cycles that would cause destruction at the corresponding magnitude of equivalent stresses. The number of cycles (Fig. 9), which a shaft could withstand, is equal to $1/D$.

To determine a shaft endurance limit, one uses a multiplier method by Marin. Then the endurance limit of a shaft is calculated [26]:

$$\sigma_e=k_a k_b k_c k_d k_e k_f \sigma'_e, \tag{3}$$

where σ'_e is the endurance limit of a material; k_a is the surface factor; k_b is the size factor; k_c is the load factor; k_d is the temperature factor; k_e is the reliability factor; k_f is the multiplier taking into consideration other effects.

To determine the endurance limit of a shaft's material σ'_e, a steel reference book is used. Following [27], the endurance limit of steel 45 when tested for torsion over a symmetrical cycle is 157 MPa. The Marin multipliers are determined from experimental studies reported in paper [25]. For hardened steel, the coefficient k_a is 0.41. The multiplier k_b for cylinders under the influence of bending and torsion loads is calculated depending on the diameter of the cylinder, and this multiplier decreases as the diameter increases. Therefore, the diameter of the cylindrical surface is used to estimate the value of this multiplier. For the cylindrical surface in question, the coefficient k_b is equal to $0.91d\ [\text{inch}]^{-0.157}=0.74$.

The multiplier k_c effect on the endurance limit has already been taken into consideration as the experimental value for endurance limit σ'_e for torsion is used. Therefore, the value k_c is taken to equal 1. The temperature factor in a given study was not taken into consideration, so the multiplier k_d is taken to equal 1. The coefficient k_e depends on the degree of reliability expected from the machine. Reliability of 95 % corresponds to the value $k_e=0.868$. Because other effects (residual stresses, corrosion, etc.) are not considered within the framework of a given study, the value of multiplier k_f is accepted equal to 1.

To determine the number of cycles N_i, formula (2) employs the following ratio [25]:

$$N_i=\left(\frac{\sigma_{rev}}{a}\right)^{\frac{1}{b}}, \tag{4}$$

where σ_{rev} is the value of the stress amplitude at a symmetrical cycle; for the selected material parameters,

$$b=-\frac{1}{3}\log\left(\frac{f\sigma}{\sigma_e}\right),\ a=\frac{(f\sigma)^2}{\sigma_e},\ f=0.79.$$

A Goodman diagram is used to reduce a load cycle to a symmetrical cycle [25]. The value for σ_{rev} is calculated as follows:

$$\sigma_{revi}=\frac{\sigma_{ai}}{1-\frac{\sigma_{mi}}{\sigma}}, \tag{5}$$

where

$$\sigma_{ai}=\frac{\sigma_{maxi}-\sigma_{mini}}{2},\ \sigma_{mi}=\frac{\sigma_{maxi}+\sigma_{mini}}{2}.$$

The values for parameters σ_{revi} and N_i for the cycle under consideration (Fig. 9) are given in Table 2.

Table 2

Parameters of symmetric cycle at different loading sections

Section number, i	σ_{revi}, MPa	N_i
1	0.570668	$3.2\cdot10^{11}$
2	0.028771	$2.22\cdot10^{15}$
3	0.243345	$3.99\cdot10^{12}$
4	0.223467	$5.14\cdot10^{12}$
5	0.830953	$1.05\cdot10^{11}$
6	0.36235	$1.23\cdot10^{12}$
7	1.309058	$2.74\cdot10^{10}$
8	1.414367	$2.18\cdot10^{10}$
9	0.013622	$2.03\cdot10^{16}$
10	0.155559	$1.5\cdot10^{13}$
11	0.917886	$7.85\cdot10^{10}$
12	1.301945	$2.79\cdot10^{10}$
13	0.307624	$2\cdot10^{12}$
14	0.811724	$1.13\cdot10^{11}$
15	0.144082	$1.88\cdot10^{13}$
16	0.226529	$4.94\cdot10^{12}$

The amount of damage to the shaft D over the entire load cycle, calculated from formula (2), is $D=1.54\cdot10^{-10}$. This corresponds to the number of load cycles equal to $6.48\cdot10^{9}$.

6. Discussion of results from studying the shaft resource

The approach to determining the resource of eccentric shafts has been proposed, which consists of a joint calculation of the dynamic stressed-deformable state of the structure and the calculation of resource based on the method of cumulative accumulation of damages. The procedure, proposed in this paper, can be generalized to involve research into elements of energy equipment, which includes internal combustion engines, steam and hydraulic turbines.

Finite-element modeling of the stressed-deformed state of a structure makes it possible to evaluate its resource without conducting a physical experiment. The accuracy of the proposed method is limited to matching the fatigue properties of a material to the Weller diagram.

The benefit of the proposed procedure is a possibility to adapt it to other classes of structures. The drawback of the proposed procedure is strong dependence of results on the mechanical characteristics of a material, which are not always known.

The level of stresses in the examined structure is too small to give rise to plastic deformations that often occur in engineering systems. In the future, it is extremely interesting to explore dynamic plastic deformations and, consequently, the low-cycle fatigue that occurs in a structure.

7. Conclusions

1. A new approach to calculating the resource of carrier shafts in eccentric mechanisms has been proposed, which includes numerical modeling of their dynamic stressed-deformed state and a procedure for calculating the resource based on cumulative accumulation of damage. Given the complexity of shaft's design, its dynamic stressed state was simulated by a finite element method using tetrahedral 3D elements at a small time step.

2. The resource of a shaft carrier in the mill CGM 140/320 has been investigated. The maximum dynamic stressed state of the shaft is observed on the cheek of the shaft near the crank. It is for this most loaded place that resource calculations are performed employing a method of cumulative accumulation of damages. The equivalent mechanical stresses in this region range from 22.498 to 27.258 MPs over a complex cycle consisting of 16 elementary sections.

References

1. Fatemi, A. (2004). Fatigue behavior and life predictions of notched specimens made of QT and forged microalloyed steels. International Journal of Fatigue, 26(6), 663–672. doi: https://doi.org/10.1016/j.ijfatigue.2003.10.005
2. Daemi, N., Majzoob, G. H. (2011). Experimental and Theoretical investigation on notched specimen's life under bending loading. International Journal of Mechanical and Mechatronics Engineering, 5 (8), 1639–1643.
3. Bader, Q., Kadum, E. (2014). Effect of V notch shape on fatigue life in steel beam made of AISI 1037. International Journal of Engineering Research and Applications, 4 (6 (6)), 39–46.
4. Zhao, L.-H., Xing, Q.-K., Wang, J.-Y., Li, S.-L., Zheng, S.-L. (2019). Failure and root cause analysis of vehicle drive shaft. Engineering Failure Analysis, 99, 225–234. doi: https://doi.org/10.1016/j.engfailanal.2019.02.025
5. Shinde, V., Jha, J., Tewari, A., Miashra, S. (2017). Modified Rainflow Counting Algorithm for Fatigue Life Calculation. Proceedings of Fatigue, Durability and Fracture Mechanics, 381–387. doi: https://doi.org/10.1007/978-981-10-6002-1_30
6. Wang, Y. (2010). Spectral fatigue analysis of a ship structural detail – A practical case study. International Journal of Fatigue, 32 (2), 310–317. doi: https://doi.org/10.1016/j.ijfatigue.2009.06.020
7. GopiReddy, L. R., Tolbert, L. M., Ozpineci, B., Pinto, J. O. P. (2015). Rainflow Algorithm-Based Lifetime Estimation of Power Semiconductors in Utility Applications. IEEE Transactions on Industry Applications, 51 (4), 3368–3375. doi: https://doi.org/10.1109/tia.2015.2407055
8. Fatemi, A., Yang, L. (1998). Cumulative fatigue damage and life prediction theories: a survey of the state of the art for homogeneous materials. International Journal of Fatigue, 20 (1), 9–34. doi: https://doi.org/10.1016/s0142-1123(97)00081-9
9. Quigley, J. P., Lee, Y.-L., Wang, L. (2016). Review and Assessment of Frequency-Based Fatigue Damage Models. SAE International Journal of Materials and Manufacturing, 9 (3), 565–577. doi: https://doi.org/10.4271/2016-01-0369
10. Ariduru, S. (2004). Fatigue life calculation by rainflow cycle counting method. Ankara.
11. Yoon, M., Kim, K., Oh, J. E., Lee, S. B., Boo, K., Kim, H. (2015). The prediction of dynamic fatigue life of multi-axial loaded system. Journal of Mechanical Science and Technology, 29 (1), 79–83. doi: https://doi.org/10.1007/s12206-014-1212-1
12. Rao, J. S. (2010). Optimized Life Using Frequency and Time Domain Approaches. IUTAM Bookseries, 13–26. doi: https://doi.org/10.1007/978-94-007-0020-8_2
13. Ragan, P., Manuel, L. (2007). Comparing Estimates of Wind Turbine Fatigue Loads Using Time-Domain and Spectral Methods. Wind Engineering, 31 (2), 83–99. doi: https://doi.org/10.1260/030952407781494494
14. Singh, A., Soni, V., Singh, A. (2014). Structural Analysis of Ladder Chassis for Higher Strength. International Journal of Emerging Technology and Advanced Engineering, 4 (2), 253–259.
15. Thriveni, K., Chandraiah, B. J. (2013). Modeling And Analysis Of The Crankshaft Using Ansys Software. International Journal of Computational Engineering Research, 3 (5), 84–89.
16. Espadafor, F. J., Villanueva, J. B., García, M. T. (2009). Analysis of a diesel generator crankshaft failure. Engineering Failure Analysis, 16 (7), 2333–2341. doi: https://doi.org/10.1016/j.engfailanal.2009.03.019

17. Fonte, M., Reis, L., Romeiro, F., Li, B., Freitas, M. (2006). The effect of steady torsion on fatigue crack growth in shafts. International Journal of Fatigue, 28 (5-6), 609–617. doi: https://doi.org/10.1016/j.ijfatigue.2005.06.051
18. SongSong, S., MaoSong, W., Hui, W., Ying, Z., Mei, X. X. (2019). Study of component high cycle bending fatigue based on a new critical distance approach. Engineering Failure Analysis, 102, 395–406. doi: https://doi.org/10.1016/j.engfailanal.2019.04.050
19. Zhu, C., He, J., Peng, J., Ren, Y., Lin, X., Zhu, M. (2019). Failure mechanism analysis on railway wheel shaft of power locomotive. Engineering Failure Analysis, 104, 25–38. doi: https://doi.org/10.1016/j.engfailanal.2019.05.013
20. Rusiński, E., Harnatkiewicz, P., Przybyłek, G., Moczko, P. (2010). Analysis of the Fatigue Fractures in the Eccentric Press Shaft. Solid State Phenomena, 165, 321–329. doi: https://doi.org/10.4028/www.scientific.net/ssp.165.321
21. Thamaraiselvan, A., Thanesh, A., Suresh, K., Palani, S. (2016). Design and Development of Reliable Integral Shaft Bearing for Water Pump in Automotive Engine to Reduce Assemble Time and Increase Production. Indian Journal of Science and Technology, 9 (1). doi: https://doi.org/10.17485/ijst/2016/v9i1/85756
22. Kurle, A., Raut, L. (2013). A Review on Design and Development of Eccentric Shaft for Cotton Ginning Machine. International Journal of Engineering Research & Technology, 2 (1).
23. Arinova, D. B., Askarov, E. S., Popov, G. (2018). Investigation and design testing of the centrifugal gyratory mill of a coulisse type. News of the National Academy of Sciences of the Republic of Kazakhstan, 2 (428), 61–71.
24. Vol'dek, A. I., Popov, V. V. (2010). Elektricheskie mashiny peremennogo toka. Sankt-Peterburg: Piter, 350.
25. Nisbett, J. K., Budynas, R. G. (2006). Shigley's Mechanical Engineering Design. New York: McGraw-Hill Education, 1109.
26. Marin, J. (1962). Mechanical Behavior of Engineering Materials. New Jersey: Prentice-Hall, 502.
27. Dragunov, Yu. G., Zubchenko, A. S., Kashirskiy, Yu. V. et. al. (2014). Marochnik staley i splavov. Moscow, 1216.